An Inverse Boundary-Layer Method for Compressible Laminar and Turbulent Boundary Layers

Tuncer Cebeci*
California State University, Long Beach, Calif.

This paper presents an efficient two-point finite-difference method for solving the compressible laminar and turbulent boundary-layer equations for a given external velocity distribution (standard problem) as well as an efficient method for solving the same equations for a prescribed positive wall shear or displacement thickness (inverse problem). In the equations the Reynolds stress terms are modeled by using the eddy-diffusivity formulas developed by Cebeci and Smith. The accuracy of the method is investigated for both incompressible and compressible turbulent flows.

Nomenclature

A = Van Driest damping length parameter
c_f = local skin-friction coefficient
C = viscosity-density parameter
f = dimensionless stream function
f' = u/u_e
g = dimensionless total-enthalpy ratio, H/H_e
h = specific enthalpy
H = total enthalpy, or shape factor, δ^*/θ, wherever applicable
K = variable grid parameter
L = modified mixing length
M = Mach number
p = pressure
p^+ = dimensionless pressure-gradient parameter
Pr = Prandtl number
Pr_t = turbulent Prandtl number
R_x = Reynolds number, $u_e x/\nu_e$
R_θ = Reynolds number, $u_e\theta/\nu_e$
u,v = velocity components in the x- and y-directions, respectively
u_τ = friction velocity $(\tau_w/\rho_w)^{1/2}$
x,y = Cartesian coordinates
α = parameter in the outer eddy viscosity formula, see Eq. (7b)
δ = boundary-layer thickness
δ^* = displacement thickness $\int_0^\infty [1-(\rho u/\rho_e u_e)]dy$
ϵ_m, ϵ_H = eddy viscosity and eddy conductivity, respectively
$\epsilon_m^+, \epsilon_H^+$ = dimensionless eddy viscosity and eddy conductivity, respectively
η = transformed y-coordinate
η_∞ = transformed boundary-layer thickness
Θ = momentum thickness, $\int_0^\infty (\rho u/\rho_e u_e)[1-(u/u_e)]dy$
κ = Von Karman's constant
μ = dynamic viscosity
ν = kinematic viscosity
ρ = density
τ = shear stress
ψ = stream function

Subscripts

e = outer edge of boundary layer
w = wall
∞ = freestream conditons
$( )'$ = differentiation with respect to η

Received February 12, 1975; revision received August 8, 1975. This work was supported by the Office of Naval Research under contract N00014-74-A-0203-001.

Index categories: Boundary Layers and Convective Heat Transfer – Laminar; Boundary Layers and Convective Heat Transfer – Turbulent.

*Adjunct Professor, Mechanical Engineering Department. Member AIAA.

I. Introduction

STUDIES in separating boundary layers leading to accurate methods for predicting flow separation, flows on the verge of separation, separating and reattaching flows, and fully separated flows find a large number of applications in aerodynamic problems and in the design of airplanes for both commercial and military applications. For example, an accurate determination of the separation point is very crucial in many problems since separation strongly influences the performance of the flow configuration under consideration. A common procedure employed to determine this point is to solve the governing boundary-layer equations for a given external velocity distribution and find the point (if any) where the wall shear goes to zero. According to recent studies (e.g., Ref. 1), such a prediction can be done accurately for two-dimensional and axisymmetric laminar and turbulent flows. Such a capability should also exist shortly for three-dimensional flows in view of the considerable work being done in this area (see, for example, Refs. 2-4).

Predicting flows on the verge of separation (that is, flows with zero wall shear) is quite important in many problems. In the case of airfoils, where it is desired to maximize the lift, it is necessary to compute the minimum distance over which a given pressure rise can be obtained without the flow separating. The most rapid pressure rise that it is possible to obtain occurs when the wall shear stress along the suction side of the airfoil approaches and is maintained near zero. Therefore, it is of considerable interest to be able to calculate boundary layers with specified values for the wall shear that also decrease to zero. The Liebeck airfoils discussed in Refs. 5 and 6 are designed on that principle.

Prediction of partially separating flows is one of the most difficult, yet rewarding tasks in aerodynamic problems. An economic and efficient operation of aerodynamic devices depends on smooth, streamlined flow. The upper limit of this efficient operating range is marked by the flow breakaway, called separation, or stall. This ideal condition is seldom attained in practice, since a design in a series of compromises between conflicting requirements. As a specific example, consider an airplane wing whose maximum lift is determined by separation. If this wing were designed from the performance standpoint alone, simultaneous spanwise stall would be desirable. However, because nobody wants to stall without lateral control (this is done by ailerons), wings are designed to have progressive stall from the wing root out. Operating with partially separated wings, especially for swept wings, creates,

in turn, longitudinal control problems because of shifts in the center of pressure. From the standpoint of design of control surfaces it is necessary to have methods for calculating overall forces on wings with partial separation. Today such a capability for calculating partially separating flows, even in two dimensions, does not exist.

Prediction of separating and reattaching flows is also very important. Two typical examples of such flows are a leading edge bubble and shock boundary-layer interaction. In both cases the boundary layer is temporarily separated from the surface but reattached a short distance afterward. Here it is important to determine under what conditions the boundary layer reattaches or separates completely. The reattachment after a leading edge bubble on highly swept wings is relative to the leading edge vortex formation, and the absence of reattachment after a shock signifies shock stall. Today a satisfactory prediction of separating and reattaching flows, even for two dimensions, again does not exist.

In recent years a number of studies on inverse boundary-layer flows have been conducted. Except for the integral-method approaches, most of these studies have been directed to laminar layers. Catherall and Mangler solved the laminar boundary-layer equations in the usual way[7] until the separation point was approached. By assuming that the displacement thickness behaves in a regular prescribed fashion in the region of the separation point, they calculated the pressure distribution in that region for the prescribed displacement thickness distribution. Their numerical solutions did not show any signs of a singular behavior at separation.

Keller and Cebeci[8] solved the laminar boundary-layer equations for a prescribed positive wall shear and, Klineberg and Steger[9] solved them for a prescribed negative wall shear. Carter[10] presented numerical solutions for the laminar boundary-layer equations involving separation and reattachment. He obtained solutions with an inverse procedure in which he prescribed the displacement thickness or the wall shear. He compared his results with Klineberg and Steger's separated boundary-layer calculations[9] and with Briley's solution[11] of the Navier-Stokes equations for a separated region.

Cebeci, Berkant, Silivri, and Keller[3] solved the turbulent boundary layer equations for a prescribed positive wall shear. The only other turbulent boundary-layer calculations for flows with prescribed wall shear were made by Kuhn and Nielsen,[13] by using an integral technique. However, unlike Ref. 12, their solutions also included negative as well as positive wall shear.

The method described in this paper is the *first* on the solution of compressible laminar and turbulent boundary layers with a prescribed positive wall shear. It provides a useful and powerful method for calculating flows on the verge of separating. It also provides a first step in calculating compressible boundary layers for separating and reattaching flows. Studies are currently being conducted to extend this method for flows with prescribed negative wall shear or with prescribed displacement thickness with flow separation.

II. Governing Equations

The governing boundary-layer equations for steady, two-dimensional, compressible, laminar and turbulent boundary layers are the continuity, momentum, and energy equations. These equations and their boundary conditions (for zero mass transfer) are:

Continuity

$$\frac{\partial}{\partial x}(\rho u)+\frac{\partial}{\partial y}(\overline{\rho v})=0 \tag{1}$$

Momentum

$$\rho u\frac{\partial u}{\partial x}+\overline{\rho v}\frac{\partial u}{\partial y}=-\frac{\mathrm{d}p}{\mathrm{d}x}+\frac{\partial}{\partial y}\left[\mu\frac{\partial u}{\partial y}-\overline{\rho u'v'}\right] \tag{2}$$

Energy

$$\rho u\frac{\partial H}{\partial x}+\overline{\rho v}\frac{\partial H}{\partial y}=\frac{\partial}{\partial y}\left[\frac{\mu}{Pr}\frac{\partial H}{\partial y}-\overline{\rho v'H'}+\mu\left(1-\frac{1}{Pr}\right)u\frac{\partial u}{\partial y}\right] \tag{3}$$

$$y=0 \quad u,v=0 \quad H=H_w \quad \text{or} \quad (\partial H/\partial y)_w=\text{given} \tag{4a}$$

$$y\to\infty \quad u\to u_e(x) \quad H\to H_e \tag{4b}$$

The solution of the system given by Eqs. (1-4) requires closure assumptions for the Reynolds stresses, $-\overline{\rho u'v'}$ and $-\overline{\rho v'H'}$. Here we satisfy these requirements by using eddy-viscosity (ϵ_m) and eddy-conductivity (ϵ_H) concepts and define them by

$$-\overline{\rho u'v'}=\rho\epsilon_m\frac{\partial u}{\partial y}, \quad -\overline{\rho v'H'}=\rho\epsilon_H\frac{\partial H}{\partial y} \tag{5}$$

and relate ϵ_m and ϵ_H to a turbulent Prandtl number Pr_t by

$$Pr_t=\epsilon_m/\epsilon_H \tag{6}$$

According to the eddy-viscosity formulation of Cebeci and Smith,[14] the turbulent boundary layer is divided into two regions, called inner and outer regions, and eddy-viscosity formulas are defined by separate formulas in each region. They are (for no mass transfer)

$$\epsilon_m\equiv(\epsilon_m)_i=L^2\left|\frac{\partial u}{\partial y}\right|, \qquad (\epsilon_m)_i\le(\epsilon_m)_0 \tag{7a}$$

$$\epsilon_m\equiv(\epsilon_m)_0=\alpha\left|\int_0^\infty(u_e-u)\,\mathrm{d}y\right|, \qquad (\epsilon_m)_0>(\epsilon_m)_i \tag{7b}$$

Here

$$L=\kappa y[1-\exp(-y/A)]$$

$$A=A^+\nu\frac{\nu}{N}\left(\frac{\tau_w}{\rho_w}\right)^{-1/2}\left(\frac{\rho}{\rho_w}\right)^{1/2}$$

$$N=[1-11.8(\mu_w/\mu_e)(\rho_e/\rho_w)^2p^+]^{1/2}$$

$$p^+=\frac{\nu_e u_e}{u_\tau^3}\frac{\mathrm{d}u_e}{\mathrm{d}x}, \qquad u_\tau=\left(\frac{\tau_w}{\rho_w}\right)^{1/2} \tag{8}$$

In Eqs. (7b) and (8) α, κ, and A^+ are "universal" constants equal to 0.0168, 0.40, and 26, respectively, for high Reynolds number flows, $R_\theta>5000$. To compute flows at low Reynolds numbers, one can modify them as discussed in Ref. 14. The eddy-viscosity formulas, Eqs. (7) can also be modified to compute transitional boundary layers as well as boundary layers in which the streamwise wall curvature becomes important. Again for a detailed discussion see Ref. 14.

III. Transformation of the Governing Equations

Before we solve the system given by Eqs. (1-4) with the Reynolds stresses replaced by Eq. (5), we introduce the Falkner-Skan transformation in order to remove the singularity at $x=0$ and to stretch the coordinates in the x- and y-directions; that is

$$x=x, \quad \mathrm{d}\eta=\left(\frac{u_e}{\rho_e\mu_e x}\right)^{1/2}\rho\,\mathrm{d}y \tag{9}$$

We also define a dimensionless stream function $f(x,\eta)$ by

$$\psi=(\rho_e\mu_e u_e x)^{1/2}f(x,\eta) \tag{10}$$

Here ψ is the usual definition of stream function that satisfies the continuity equation. With the relations in Eqs. (9) and (10), we can write the momentum and energy equations as

Momentum

$$(bf'')' + P_1 ff'' + P_2[c-(f')^2] = x\left(f'\frac{\partial f'}{\partial x} - f''\frac{\partial f}{\partial x}\right) \quad (11)$$

Energy

$$(eg' + df'f'')' + P_1 fg' = x\left(f'\frac{\partial g}{\partial x} - g'\frac{\partial f}{\partial x}\right) \quad (12)$$

where primes denote differentiation with respect to η and

$$f' = \frac{u}{u_e}, \quad g \equiv \frac{H}{H_e}, \quad c = \frac{\rho_e}{\rho}, \quad C \equiv \frac{\rho\mu}{\rho_e\mu_e} \quad (13a)$$

$$b = (1+\epsilon_m^+)C, \quad e = \frac{C}{Pr}\left(1+\epsilon_m^+\frac{Pr}{Pr_t}\right), \quad d = \frac{u_e^2}{H_e}\left(1-\frac{1}{Pr}\right) \quad (13b)$$

$$P_1 \equiv \frac{1}{2}\left[1+P_2+\frac{x}{\rho_e\mu_e}\frac{\mathrm{d}}{\mathrm{d}x}(\rho_e\mu_e)\right], \quad P_2 = \frac{x}{u_e}\frac{\mathrm{d}u_e}{\mathrm{d}x} \quad (13c)$$

Similarly the boundary conditions in Eq. (4) become

Momentum

$$\eta = 0 \qquad f = 0 \qquad f' = 0 \quad (14a)$$

$$\eta = \infty \qquad f' = 1 \quad (14b)$$

Energy

$$\eta = 0 \qquad g = g_w \quad \text{or} \quad g_w' = \text{given} \quad (15a)$$

$$\eta = \infty \qquad g = 1 \quad (15b)$$

In terms of transformed variables, the inner and outer eddy viscosity formulas can also be transformed, as is discussed in Ref. 15.

IV. Standard and Inverse Problems

The system given by Eqs. (11), (12), (14), and (15) with specified $u_e(x)$ or $P_2(x)$ is the typical two-dimensional boundary-layer problem for laminar and turbulent flows. For convenience we shall call it the *standard problem*.

There are a number of problems that require inverse procedures in viscous flows. One type of *inverse problem* results from requiring that the local skin-friction coefficient c_f defined by

$$c_f = \frac{\tau_w}{(1/2)\rho_e u_e^2} \quad (16)$$

be specified. Another type of inverse problem results from requiring that the displacement thickness defined by

$$\delta^* = \int_0^\infty \left(1-\frac{\rho u}{\rho_e u_e}\right)\mathrm{d}y \quad (17)$$

be specified. Other inverse problems can be formulated as discussed in Ref. 15.

Let us consider the case in which c_f is specified, and write Eq. (16) in terms of transformed variables

$$c_f = 2f_w'' C_w/\sqrt{R}_x \quad (18)$$

The system given by Eqs. (11), (12), (14), (15), and (18) is overdetermined, and we cannot specify $P_2(x)$ (i.e., $u_e(x)$) arbitrarily. Rather we must determine $P_2(x)$ as well as $f(x,\eta)$ to solve the system. In the case of specified δ^*, we replace Eq. (18) with the transformed form of Eq. (17); that is,

$$\delta^* = \frac{x}{\sqrt{R}_x}\int_0^{\eta_\infty}\left(\frac{\rho_e}{\rho} - f'\right)\mathrm{d}\eta \quad (19)$$

V. Newton's Method for the Inverse Problem

To describe our numerical approach to the problem for the *specified c_f case*, let us assume that at $x = x_{n-1}$ we are given the profiles of f, f', f'', g, g', the velocity gradient $P_2(x_{n-1})$, and the velocity $u_e(x_{n-1})$. At $x = x_n$ we seek an accurate approximation to the solution of Eqs. (11) and (12) subject to Eqs. (14) and (15) for a given $c_f(x)$. To start the calculations, it is necessary to know $P_2(x)$ and $u_e(x)$. The latter is necessary since R_x is a function of u_e. In our method we assume $P_2(x)$ and calculate $u_e(x)$ from the definition of $P_2(x)$ in Eq. (13c). Using central differences we approximate P_2 and solve it for $u_e^n = u_e(x_n)$ to get

$$u_e^n = -u_e^{n-1}\frac{P_2^{n-1/2}+2\alpha_n}{P_2^{n-1/2}-2\alpha_n} \quad (20)$$

where

$$\alpha_n = \frac{x_{n-1/2}}{x_n - x_{n-1}}, \quad P_2^{n-1/2} = \frac{1}{2}(P_2^n + P_2^{n-1}),$$

$$x_{n-1/2} = \frac{1}{2}(x_n + x_{n-1}) \quad (21)$$

Once $P_2(x)$ and $u_e(x)$ are known, then the standard problem Eqs. (11) and (12) subject to Eqs. (14) and (15), can be solved. The numerical method used to do this will be described in Sec. VI. Let us denote the solution of the standard problem by

$$f(x,\eta) = \beta[x,\eta,P_2(x)] \quad (22)$$

Using this solution, we can now calculate c_f (which we shall denote by c_{f_c}) from Eq. (18). Recalling that the desired value for the skin-friction coefficient is $c_f(x)$, we form:

$$\phi[P_2(x)] \equiv c_{f_c} - c_f \quad (23)$$

and seek $P_2(x)$ such that $\phi[P_2(x)] = 0$ for $x > 0$.

To solve $\phi[P_2(x)] = 0$, we use Newton's method. With some estimate $P_2^{(\nu)}(x)$ of the desired pressure gradient, we define the sequence $P_2^{(\nu)}(x)$ by setting

$$P_2^{\nu+1}(x) = P_2^{\nu}(x) - \frac{\phi[P_2^{(\nu)}(x)]}{(\partial/\partial P_2)\{\phi[P_2^{(\nu)}(x)]\}} \quad (24)$$

The derivative of ϕ with respect to P_2 can be obtained from Eq. (23) by making use of the relation given by Eqs. (18) and (20). This gives

$$\frac{\partial\phi}{\partial P_2} = \frac{2C_w}{\sqrt{R}_x}\left\{-F_w'' + f_w''\frac{u_e^{n-1}}{u_e^n}\left[\frac{2\alpha_n}{(P_2^{n-1/2}-2\alpha_n)^2}\right]\right\} \quad (25)$$

where

$$F_w'' = \partial f_w''/\partial P_2 \quad (26)$$

To summarize one step of iteration of Newton's method, we first estimate a value for $P_2(x_n)$, then calculate u_e^n from Eq. (20), and obtain a solution of Eqs. (11) and (12) subject to Eqs. (14) and (15). The solution yields a $c_{f_c}^{(\nu)}$ according to Eq. (18). From this result and from the desired value $c_f(x_n)$, we

find ϕ from Eq. (23). It is then clear that the next value of $P_2(x_n)\,[\equiv P_2^{(\nu+1)}(x_n)]$ can be calculated from Eq. (24), provided that $\partial\phi/\partial P_2$ is known. (We shall discuss its calculation later.) The iteration process is repeated until

$$|P_2^{(\nu+1)}(x_n) - P_2^{(\nu)}(x_n)| < \gamma_1 \tag{27}$$

where γ_1 is a small error tolerance.

Our procedure for the *specified* δ^* *case* is similar to the procedure for the specified c_f case. The difference in the procedure starts after we get the solution denoted by Eq. (22). Denoting the calculated value of δ^* by δ_c^*, and the desired value by δ^*, we form

$$\phi[P_2(x)] \equiv \delta_c^* - \delta^* \tag{28}$$

We obtain $P_2^{\nu+1}(x)$ from the expression given by Eq. (24). To find the derivative of ϕ with respect to P_2 from Eq. (28), we first write Eq. (19) as

$$\delta^* = xA/\sqrt{R_x} \tag{29}$$

where

$$A \equiv \int_0^\infty (c-u)\,d\eta \tag{30}$$

Differentiating Eq. (29) with respect to P_2 and using Eq. (28), we get

$$\frac{\partial\phi}{\partial P_2} = \frac{x}{\sqrt{R_x}}\left[\frac{\partial A}{\partial P_2} - \frac{A}{2}\,\frac{1}{u_e^n}\,\frac{\partial u_e}{\partial P_2}\right] \tag{31}$$

From Eqs. (20) and (30) it follows that

$$\frac{\partial u_e}{\partial P_2} = -u_e^{n-1}\,\frac{4\alpha_n}{(P_2^{n+(1/2)} - 2\alpha_n)^2} \tag{32}$$

$$\frac{\partial A}{\partial P_2} = -F(\eta_\infty) \tag{33}$$

where $F \equiv \partial f/\partial P_2$.

VI. Solution of the Governing Equations for the Standard Problem

We use a very efficient and accurate numerical method to solve the governing equations. This is a two-point finite difference method developed by H. B. Keller[16] and applied to the boundary-layer equations by Keller and Cebeci (see, for example, Refs. 17 and 18).

According to this method we introduce new dependent variables $u(x,\eta)$, $v(x,\eta)$, $t(x,\eta)$ so that Eqs. (11) and (12) can be written as a first-order system

$$f' = u \tag{34a}$$

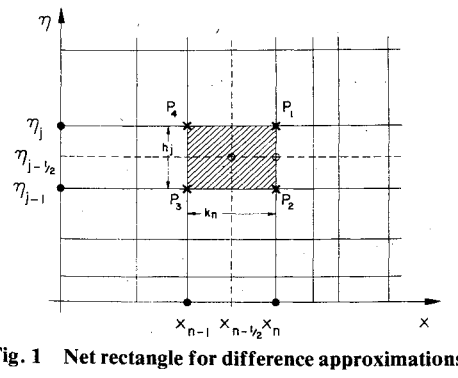

Fig. 1 Net rectangle for difference approximations.

$$u' = v \tag{34b}$$

$$g' = t \tag{34c}$$

$$(bv)' + P_1 fv + P_2(c-u^2) = x\left(u\frac{\partial u}{\partial x} - v\frac{\partial f}{\partial x}\right) \tag{34d}$$

$$(et + duv)' + P_1 ft = x\left(u\frac{\partial g}{\partial x} - t\frac{\partial f}{\partial x}\right) \tag{34e}$$

On the net rectangle shown in Fig. 1, we denote the net points by

$$x_0 = 0, \qquad x_n = x_{n-1} + k_n, \qquad n = 1,2,\ldots,N$$

$$\eta_0 = 0, \qquad \eta_j = \eta_{j-1} + h_j, \qquad j = 1,2,\ldots,J:\ \eta_J = \eta_\infty \tag{35}$$

The difference equations that are to approximate Eqs. (34) are formulated by considering one mesh rectangle, as in Fig. 1. We approximate Eqs. (34a,b,c) using centered difference quotients and average about the midpoint $(x_n, \eta_{j-1/2})$ of the segment P_1P_2 as follows

$$h_j^{-1}\,(f_j^n - f_{j-1}^n) = u_{j-1/2}^n \tag{36a}$$

$$h_j^{-1}\,(u_j^n - u_{j-1}^n) = v_{j-1/2}^n \tag{36b}$$

$$h_j^{-1}\,(g_j^n - g_{j-1}^n) = t_{j-1/2}^n \tag{36c}$$

Similarly Eqs. (34d,e) are approximated by centering about the midpoint $(x_{n-1/2}, \eta_{j-1/2})$ of the rectangle $P_1P_2P_3P_4$

$$\begin{aligned} &h_j^{-1}\,(b_j^n v_j^n - b_{j-1}^n v_{j-1}^n) + (P_1^n + \alpha_n)\,(fv)_{j-1/2}^n \\ &\quad - (P_2^n + \alpha_n)\,(u^2)_{j-1/2}^n + \alpha_n\,(v_{j-1/2}^{n-1} f_{j-1/2}^n - f_{j-1/2}^{n-1} v_{j-1/2}^n) \\ &\quad = R_{j-1/2}^{n-1} - P_2^n\,c_{j-1/2}^n \end{aligned} \tag{36d}$$

$$\begin{aligned} &h_j^{-1}\,(e_j^n t_j^n - e_{j-1}^n t_{j-1}^n) + (P_1^n + \alpha_n)\,(ft)_{j-1/2}^n \\ &\quad - \alpha_n\Big[(ug)_{j-1/2}^n + u_{j-1/2}^{n-1} g_{j-1/2}^n - g_{j-1/2}^{n-1} u_{j-1/2}^n \\ &\quad + f_{j-1/2}^{n-1}\,t_{j-1/2}^n - t_{j-1/2}^{n-1} f_{j-1/2}^n\Big] = T_{j-1/2}^{n-1} \end{aligned} \tag{36e}$$

where

$$\begin{aligned} R_{j-1/2}^{n-1} &= \alpha_n\,(fv)_{j-1/2}^{n-1} - \Big\{h_j^{-1}\,(b_j^{n-1} v_j^{n-1} - b_{j-1}^{n-1} v_{j-1}^{n-1}) \\ &\quad + P_1^{n-1}\,(fv)_{j-1/2}^{n-1} + P_2^{n-1}\Big[c_{j-1/2}^{n-1} - (u^2)_{j-1/2}^{n-1}\Big]\Big\} \end{aligned} \tag{37a}$$

$$\begin{aligned} T_{j-}^{n-1} &= \alpha_n\Big[(ft)_{j-1/2}^{n-1} - (ug)_{j-1/2}^{n-1}\Big] - 2\Big[(duv)'\Big]_{j-1/2}^{n-1/2} \\ &\quad - \Big[h_j^{-1}\,(e_j^{n-1} t_j^{n-1} - e_{j-1}^{n-1} t_{j-1}^{n-1}) + P_1^{n-1}\,(ft)_{j-1/2}^{n-1}\Big] \end{aligned} \tag{37b}$$

Equations (36) are imposed for $j = 1,2,\ldots,J$. The boundary conditions, Eqs. (14) and (15), yield, at $x = x_n$

$$f_0^n = 0, \quad u_0^n = 0, \quad u_j^n = 1, \quad g_0^n = g_w^n \quad \text{or} \quad t_0^n = t_w^n, \quad g_j^n = 1 \tag{38}$$

If we assume $(f_j^{n-1}, u_j^{n-1}, v_j^{n-1}, g_j^{n-1}, t_j^{n-1})$ to be known for $0 \le j \le J$, then Eqs. (36) for $1 \le j \le J$ and the boundary conditions Eq. (38) yield a nonlinear algebraic system of $5J+5$ equations in as many unknowns $(f_j^n, u_j^n, v_j^n, g_j^n, t_j^n)$. We use Newton's method to linearize the resulting system. The linear system is then solved by the block elimination method discussed by Isaacson and Keller.[19] For details, the reader is referred to Ref. 15.

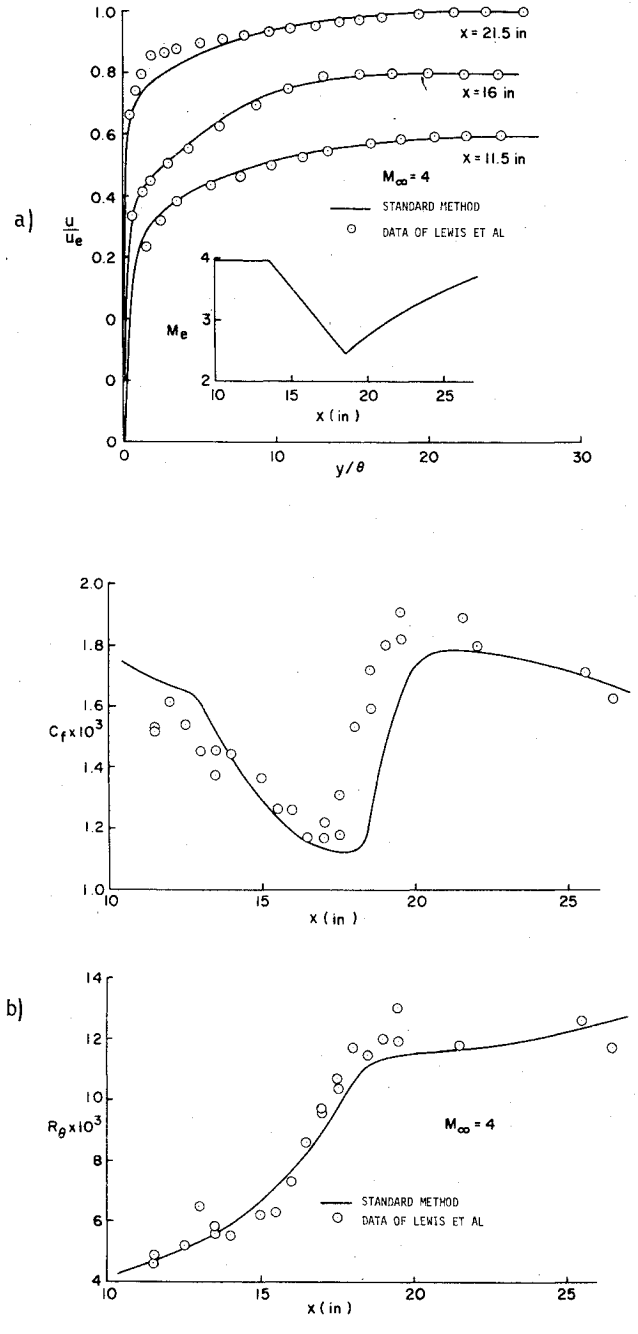

Fig. 2 Comparison of calculated and experimental results for the experimental data of Lewis et al. a) Velocity profiles and external Mach number distribution. b) Local skin-friction coefficient c_f and Reynolds number, R_θ distribution.

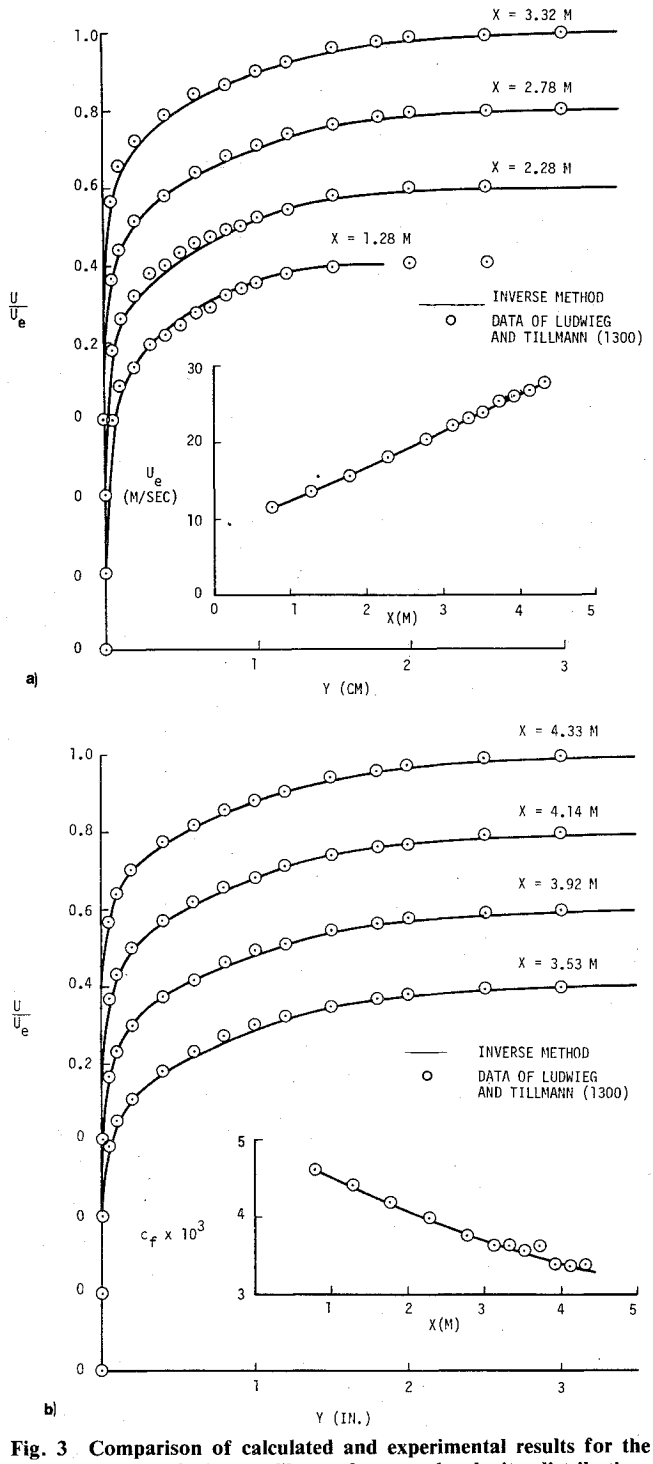

Fig. 3 Comparison of calculated and experimental results for the flow 1300. a) Velocity profiles and external velocity distribution. b) Velocity profiles and local skin-friction-coefficient distribution.

VII. Solution of the Governing Equations for the Inverse Problem

In order to calculate $\partial\phi/\partial P_2$ in Eq. (25) or Eq. (31) it is necessary to know F_w'' for the specified c_f case or $F(\eta_\infty)$ [$\equiv \partial f/\partial P_2(\eta_\infty)$] for the specified δ^* case. For this reason we take the derivative of Eqs. (36) with respect to P_2. This leads to the following linear difference equations, known as the variational equations for Eqs. (36)

$$h_j^{-1}(F_j^n - F_{j-1}^n) = U_{j-1/2}^n \tag{39a}$$

$$h_j^{-1}(U_j^n - U_{j-1}^n) = V_{j-1/2}^n \tag{39b}$$

$$h_j^{-1}(G_j^n - G_{j-1}^n) = T_{j-1/2}^n \tag{39c}$$

$$h_j^{-1}(b_j^n V_j^n - b_{j-1}^n V_{j-1}^n) + \frac{1}{2}(P_1^n + \alpha_n)$$

$$\times\left[f_j^n V_j^n + v_j^n F_j^n + f_{j-1}^n V_{j-1}^n + v_{j-1}^n F_{j-1}^n\right]$$

$$+\frac{1}{2}(fv)_{j-1/2}^n - (u^2)_{j-1/2}^n - (P_2^n + \alpha_n)(u_j^n U_j^n + u_{j-1} U_{j-1}^n)$$

$$+\frac{\alpha_n}{2}\left[v_{j-1/2}^{n-1}(F_j^n + F_{j-1}^n) - f_{j-1/2}^{n-1}(V_j^n + V_{j-1}^n)\right] = -e_{j-1/2}^n \tag{39d}$$

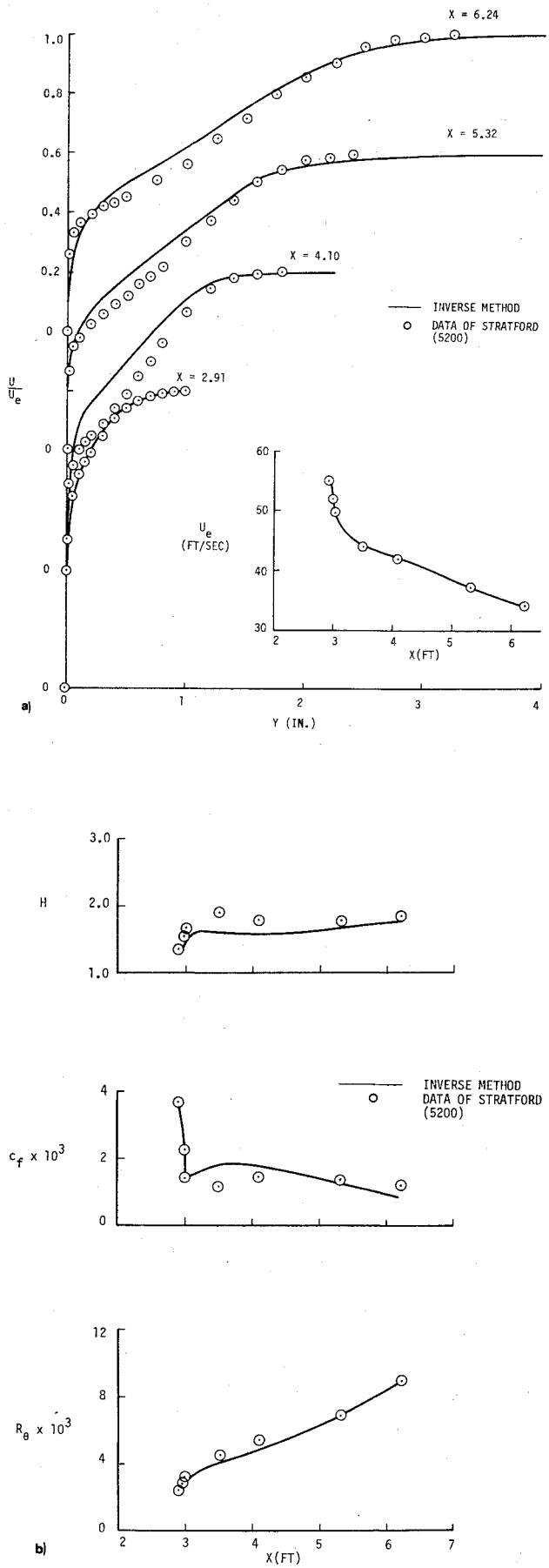

Fig. 4 Comparison of calculated and experimental results for the flow 5200. a) Velocity profiles and external velocity distribution. b) Shape factor, H, local skin-friction coefficient c_f and Reynolds number, R_θ distribution.

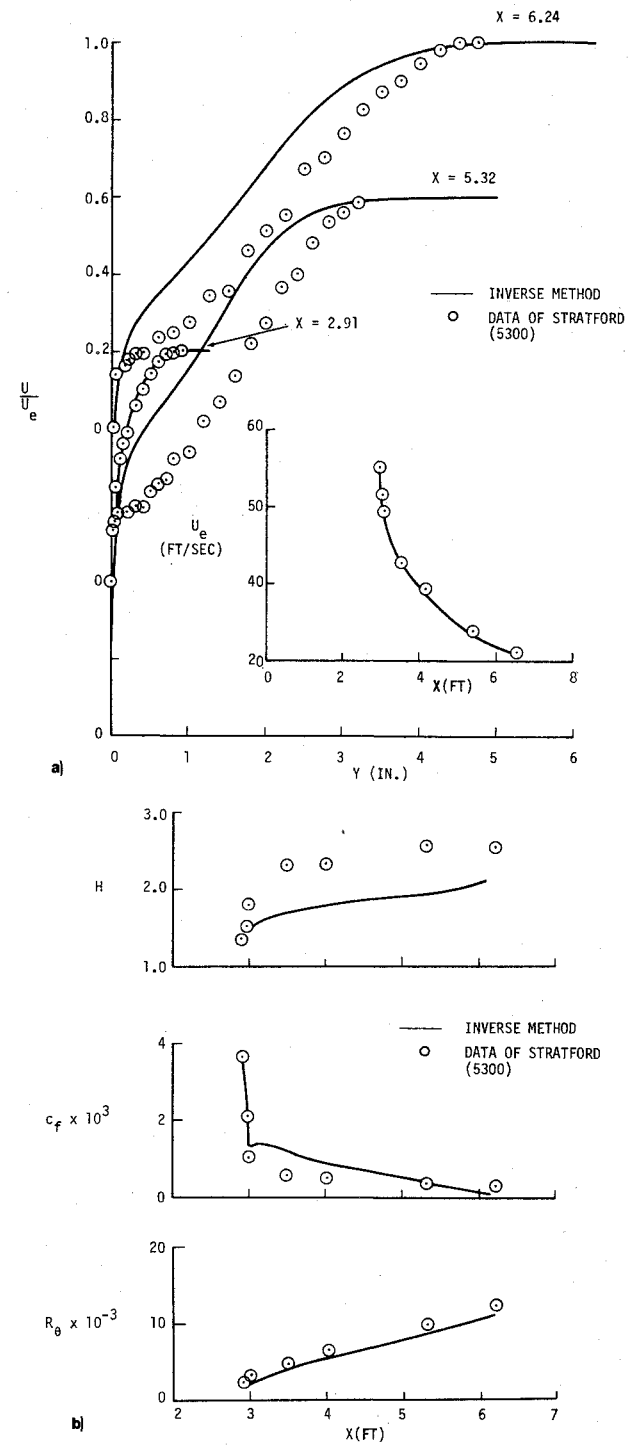

Fig. 5 Comparison of calculated and experimental results for the flow 5300. a) Velocity profiles and external velocity distribution. b) Shape factor, H, local skin-friction coefficient c_f and Reynolds number, R_θ distribution.

$$h_j^{-1}(e_j^n T_j^n - e_{j-1}^n T_{j-1}^n) + \frac{1}{2}(P_j^n + \alpha_n) \times \left[f_j^n T_j^n + t_j^n F^n{}_j + f_{j-1}^n T_{j-1}^n + t_{j-1}^n F_{j-1}^n\right] + \frac{1}{2}(ft)^n_{j-1/2} - \frac{\alpha_n}{2}\left[u_j^n G_j^n + g_j^n U_j^n + u_{j-1}^n G_{j-1}^n + g_{j-1}^n U_{j-1}^n + u_{j-1/2}^{n-1}(G_j^n + G_{j-1}^n) - g_{j-1/2}^{n-1}(U_j^n + U_{j-1}^n) + f_{j-1/2}^{n-1}(T_j^n + T_{j-1}^n) - t_{j-1/2}^{n-1}(F_j^n + F_{j-1}^n)\right] = 0 \qquad (39e)$$

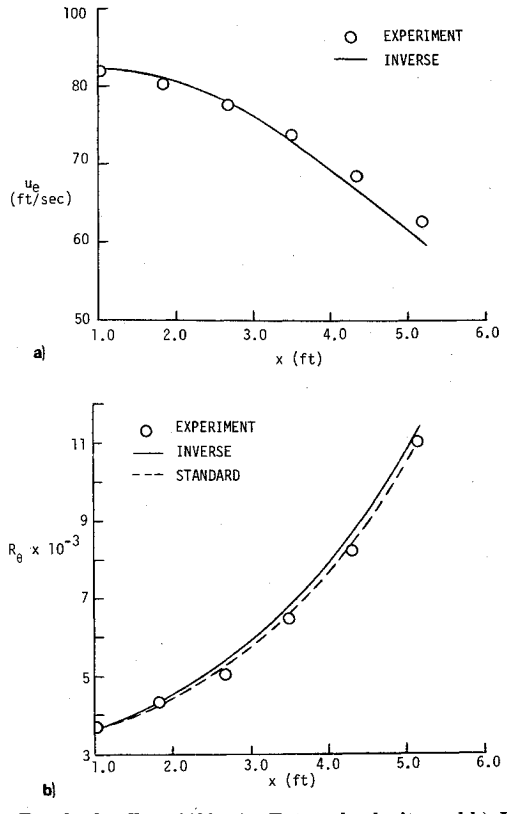

Fig. 6 Results for flow 4400. a) External velocity and b) Reynolds number, R_θ, distributions.

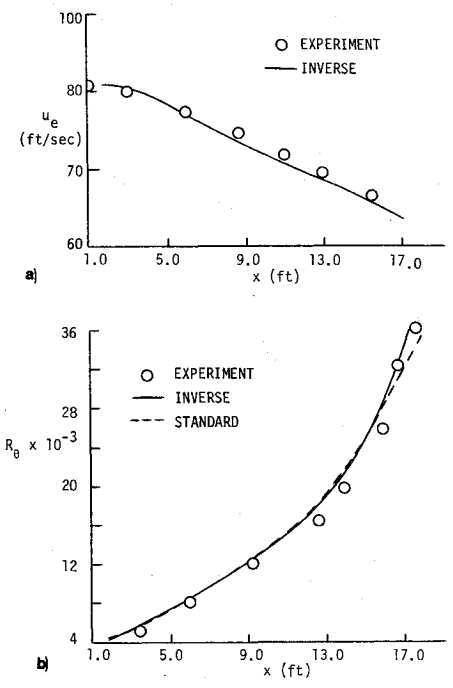

Fig. 7 Results for flow 4800. a) External velocity and b) Reynolds number, R_θ, distributions.

Similarly the boundary conditions of Eq. (38) become

$$F_0^n=0, \quad U_0^n=0, \quad U_j^n=0, \quad G_0^n=0 \text{ or } T_0^n=0 \quad G_j^n=0 \tag{40}$$

The system in Eqs. (39) and (40) again forms a block tridiagonal system (with 5×5 blocks) that is easily solved by the block elimination method described by Isaacson and Keller.[19] (See also Ref. 15 for details.)

VIII. Results for Standard and Inverse Problems

While the numerical scheme employed here is a general one in that any type of grid can be used in the η-direction (also in the x-direction), we have chosen a grid previously used by the author and his associates.[14] This grid has the property that the ratio of lengths of any two adjacent intervals is a constant, that is

$$h_j = Kh_{j-1} \tag{41}$$

The distance to the jth η-line is given by the following formula

$$\eta_j = h_1 \frac{K^j-1}{K-1} \qquad j=1,2,3,\ldots,J \quad K>1 \tag{42}$$

There are two parameters: h_1, the length of the first $\Delta\eta$-step, and K, the ratio of two successive steps. The total number of points J are calculated by the following formula

$$J=\frac{\ln[1+(K-1)\eta_\infty/h_1]}{\ln K} \tag{43}$$

To test the method for the *standard problem* we made calculations for the experimental data of Lewis et al.,[20] which consists of compressible adiabatic turbulent boundary layers in adverse and favorable pressure gradients. The results are shown in Fig. 2. The calculations were started by matching a zero-pressure-gradient profile ($R_\theta=4870$) at $x=11.5$ in. downstream of the leading edge of the model. Then the experimental Mach-number distribution shown in Fig. 2a was used to compute the rest of the flow. In general, the calculated velocity profiles, local skin friction, and momentum thickness Reynolds number values are in good agreement with experiment. We should point out here that the experimental skin-friction values were obtained by Stanton tube and were not deduced from the experimental velocity profiles.

To test our method for the inverse problem for the case of specified c_f, we made calculations for incompressible turbulent boundary layers, and checked the results obtained earlier in another study. We have chosen two experimental incompressible flows from the data reported at the Stanford Conference on Computation of Turbulent Boundary Layers.[21] In that conference the flows we have considered are known as 1300, 5200, and 5300.

Flow 1300 corresponds to an accelerating flow. The experimental data are due to Ludwieg and Tillmann. Flows 5200 and 5300 correspond to decelerating flows measured by Stratford. They differ from those more common decelerating turbulent flows in that they have a negligible skin friction. Thus, they are on the verge of separating. For this reason it is a very severe test for a numerical method and for exploring the accuracy of the eddy-viscosity formulas. In the 1968 Stanford Conference, of those that used differential methods, only *one* computed 5200 and *none* has computed 5300. The accuracy of computing these flows is also important in many design problems, as was discussed in the introduction. The Liebeck airfoils discussed in Refs. 5 and 6 are designed on these principles.

In making these computations we have first considered the standard problem. That is, for the given experimental velocity distribution and for the given initial velocity profiles at $x=x_0$, we have computed the velocity profiles and the local skin-friction coefficient at each specified x-direction. Then we made the calculations for the inverse problem. We specified the computed local skin-friction coefficient as an additional boundary condition at each x-station and computed the velocity distribution by the inverse problem. We have thus used the computed skin-friction values, rather than the experimental values, as a boundary condition. Such a procedure is necessary because a slight error in the experimental skin-friction coefficient will severely affect the computed velocity

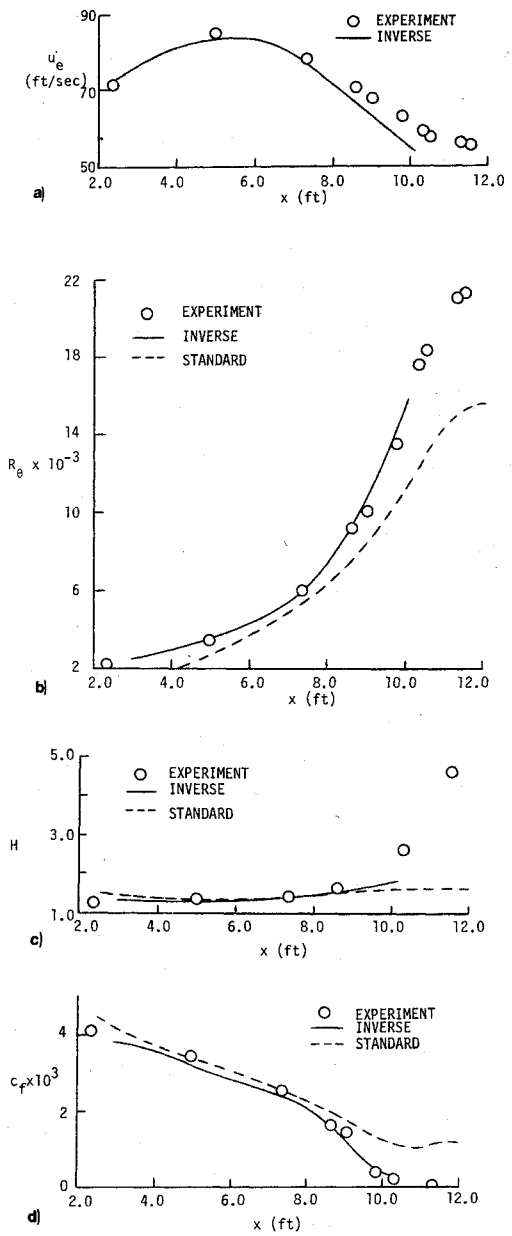

Fig. 8 Results for a separating flow experiment of Simpson and Strickland. a) External velocity, b) Reynolds number, R_θ, c) Shape factor, H, d) Local skin-friction coefficient, c_f, distributions.

distribution. To discuss this point further, let us consider the data of Stratford, both 5200 and 5300. It may be seen from the skin-friction plots in Fig. 4b and 5b that the experimental values of c_f show scatter; in an adverse pressure gradient flow, c_f should either stay nearly constant or decrease. If one uses the scattered values as inputs and computes the velocity distribution, one would get slight increases and decreases in velocity distribution with increasing and decreasing c_f, respectively.

The computed results in Fig. 3 for the accelerating flow 1300 show very good agreement with experimental data. This indicates that our eddy-viscosity formulation is quite satisfactory for this flow. On the other hand, the computed results in Figs. 4 and 5 for the two decelerating, on-the-verge-of-separating flows, 5200 and 5300, are *not satisfactory at all* although the computed results at the beginning of these two flows agree well with experiment (see the velocity profiles at $x=2.9075$ for both 5200 and 5300). This is probably due to the effect of the strong pressure gradient suddenly imposed at $x \geq 3.0$ or to the inaccuracy of the experimental data.

To further test our inverse method for flows with adverse pressure gradient, we have considered three more test cases. Of these cases, two were measured by Schubauer and Spangenberg.[21] At the 1968 Stanford Conference, these flows were labeled as 4400 and 4800. Flow 4400 has a very strong pressure gradient and flow 4800 has a mild pressure gradient.

Figures 6 and 7 show the results for flows 4400 and 4800. The calculations were made first by using the standard procedure: in this case we specified the external velocity distribution and computed the boundary-layer parameters. Next, the calculations were made by using the inverse procedure: the measured *displacement thickness* distribution was specified and the external velocity distribution was computed along with other boundary-layer parameters.

As the results show, the agreement is very good with experiment; the difference between calculated and experimental velocity distributions is relatively small, and the boundary-layer parameters computed with both procedures agree with each other.

The results for flow 4400 are quite interesting, and raise some questions about flows 5200 and 5300, since flow 4400 corresponds to a flow (like 5200 and 5300) which was on the verge of separation (negligible wall shear). Perhaps this disagreement between experiment and calculations is not due to our eddy-viscosity formulation but to the inaccuracy of the experimental data.

The third test case (see Fig. 8) we have considered corresponds to a flow with separation. The data were recently taken by Simpson and Strickland[22] on an airfoil. Flow separation was observed at $x \simeq 10.8$ ft. According to Ref. 22, for this flow the current theoretical prediction methods do not do well.

cases; calculations were made for the standard problem with specified external velocity distribution and for the inverse problem with specified displacement-thickness distribution. It is quite interesting to note that the calculated results obtained by the inverse procedure agree better with the experiment than those obtained by the standard procedure.

References

[1] Cebeci, T., Mosinskis, G. J., and Smith, A. M. O., "Calculation of Separation Points in Turbulent Flows," *Journal of Aircraft*, Vol. 9, Sept. 1972, pp. 618-624.

[2] Cebeci, T., "Calculation of Three-Dimensional Boundary Layers. I. Swept Infinite Cylinders and Small Cross Flow," *AIAA Journal*, Vol. 12, June 1974, pp. 779-786.

[3] Cebeci, T., Kaups, K., Mosinskis, G. J., and Rehn, J. A., "Some Problems of the Calculation of Three-Dimensional Boundary-Layer Flows on General Configurations," NASA CR-2285, July 1973.

[4] Cebeci, T., "Calculation of Three-Dimensional Boundary Layers," *AIAA Journal*, Vol. 13, Aug. 1975, pp. 1056-1064.

[5] Liebeck, R. H. and Ormsbee, A. I., "Optimization of Airfoils for Maximum Lift," *Journal of Aircraft*, Vol. 7, Sept.-Oct. 1970, pp. 409-415.

[6] Liebeck, R. H., "A Class of Airfoils Designed for High Lift in Incompressible Flow," *Journal of Aircraft*, Vol. 10, Oct. 1973, pp. 610-671.

[7] Catherall, D. and Mangler, K. W., "The Integration of the Two-Dimensional Laminar Boundary-Layer Equations Past the Point of Vanishing Skin Friction," *Journal of Fluid Mechanics*, Vol. 26, Pt. 1, 1966, pp. 163-182.

[8] Keller, H. B. and Cebeci, T., "An Inverse Problem in Boundary-Layer Flows: Numerical Determination of Pressure Gradient for a Given Wall Shear," *Journal of Computational Physics*, Vol. 10, No. 1, Aug. 1972.

[9] Klineberg, J. M. and Steger, J. L., "On Laminar Boundary-Layer Separation," AIAA Paper 74-94, Washington, D.C., Jan. 1974.

[10] Carter, J. E., "Solutions for Laminar Boundary Layers with Separation and Reattachment," AIAA Paper 74-583, Palo Alto, Calif., June 1974.

[11] Briley, W. R., "A Numerical Study of Laminar Separation Bubbles Using the Navier-Stokes Equations," *Journal of Fluid Mechanics*, Vol. 47, Pt. 4, 1971, pp. 713-736.

[12]Cebeci, T., Berkant, N., Silivri, I., and Keller, H. B., "Turbulent Boundary Layers with Assigned Wall Shear," to appear in *Computers and Fluids*, Vol. 3, pp. 37-49, 1975.

[13]Kuhn, G. D. and Nielsen, J. N., "Prediction of Turbulent Separated Boundary Layers," *AIAA Journal*, Vol. 12, July 1974, pp. 881-882.

[14]Cebeci, T. and Smith, A. M. O., *Analysis of Turbulent Boundary Layers*, Academic Press, New York, 1974.

[15]Cebeci, T., "An Inverse Boundary-Layer Method for Compressible Laminar and Turbulent Boundary Layers," California State Univ. at Long Beach, Rept. No. TR-74-1, Dec. 1974.

[16]Keller, H. B., "A New Difference Scheme for Parabolic Problems," *Numerical Solution of Partial Differential Equations*, edited by J. Bramble, Vol. II, Academic Press, New York, 1970.

[17]Keller, H. B. and Cebeci, T., "Accurate Numerical Methods for Boundary Layer Flows. II. Two-Dimensional Turbulent Flows," *AIAA Journal*, Vol. 10, Sept. 1972, pp. 1193-1200.

[18]Cebeci, T. and Keller, H. B., "Laminar Boundary Layers with Assigned Wall Shear," Proceedings of the *Third International Conf. on Numerical Methods in Fluid Dynamics*, Paris, France, July 1972.

[19]Isaacson, E. and Keller, H. B., *Analysis of Numerical Methods*, Wiley, New York, p. 58.

[20]Lewis, J. E., Gram, R. L., and Kuboto, T., "An Experiment in the Adiabatic Compressible Turbulent Boundary Layer in Adverse and Favorable Pressure Gradients," *Journal of Fluid Mechanics*, Vol. 51, p. 657, 1972.

[21]Coles, D. E. and Hirst, E. A., "Proceedings of Computation of Turbulent Boundary Layers," 1968 AFOSR-IFP-Stanford Conf., Vol. 2, Thermosciences Div., Stanford University, Stanford, Calif., 1969.

[22]Simpson, R. L. and Strickland, T. H., "Laser and Hot-Film Anemometer Measurements in a Separating Turbulent Boundary Layer," Tech. Rept. Southern Methodist University, Dallas, Texas, Tech. Rept. WT-3, Sept. 1974.